SUPPLEMENTARY MATERIAL TO THE ARTICLE:

Para versus *Meta* Substituents as a Means of Directing Magnetic Anisotropy in Fe_2Dy_2 Coordination Clusters

Authors: Amer Baniodeh, Valeriu Mereacre, Nicola Magnani, Yanhua Lan, Juliusz Wolny, Volker Schünemann, Christopher E. Anson, Annie K. Powell

Compounds **1** and **2** and the starting materials can be obtained as reported in V. Mereacre, A. Baniodeh, C. E. Anson, A. K. Powell, *J. Am. Chem. Soc.* **2011**, *133*, 15335.

$[Fe_2Dy_2(\mu_3\text{-}OH)_2(Htea)_2(m\text{-}NCC_6H_4CO_2)_6]\cdot 2MeCN$ (3)

$[Fe_3O(m\text{-}CNC_6H_4CO_2)_6(H_2O)_3](m\text{-}CNC_6H_4CO_2)$ (0.288 g, 0.242 mmol), triethanolamine (0.298 g, 2 mmol) and $Dy(NO_3)_3\cdot 6H_2O$ (0.116 g, 0.25 mmol) were dissolved in MeCN/MeOH (10/10 mL). The mixture was reacted for 30 min. at 80°C. The yellow solution was then left in air undisturbed. After 3 days small block-like pale-yellow crystals were collected in 13% yield.
Anal. Calc. for $C_{63}H_{58.5}Dy_2Fe_2N_{9.5}O_{21}$ (replacement of ½MeCN by H_2O): C 43.86, H 3.39, N 7.72; found: C 43.95, H 3.40, N 7.64%. Selected IR data (cm^{-1}): 3502 (br), 3077 (w), 2878 (m), 2231 (s), 1993 (w), 1773 (w), 1610 (s), 1556 (s), 1479 (w), 1459 (w), 1433 (s), 1377 (s), 1280 and 1267 (w), 1208 (m), 1165 (w), 1083 (s), 1067 (s), 1034 and 1018 (w), 921 (m), 904 (s), 831 (w), 790 (m), 789 (s), 682 and 670 (m), 599 (s), 564 (m), 490 (w), 462 (m), 410 (w).

Preparation of $[Fe_2Dy_2(\mu_3\text{-}OH)_2(teaH)_2(m\text{-}CH_3C_6H_4CO_2)_6]\cdot 2MeCN\cdot 2MeOH$ (4)

$[Fe_3O(m\text{-}CH_3C_6H_4CO_2)_6(H_2O)_3](m\text{-}CH_3C_6H_4CO_2)$ (0.273 g, 0.25 mmol), $teaH_3$ (0.298 g, 2 mmol) and $Dy(NO_3)_3\cdot 6H_2O$ (0.116 g, 0.25 mmol) were dissolved in MeCN (20 mL) and stirred at room temperature for 30 min then at 50°C for 5 min. The clear yellow-orange solution was left undisturbed in air. After 8 days pale-yellow blocks were collected in 22% yield.
Anal. Calc. for $C_{62}H_{78}Dy_2Fe_2N_2O_{22}$ (loss of 2MeCN): C 45.31, H 4.75, N 1.71; found: C 45.11, H 5.03, N 1.57%. Selected IR data (cm^{-1}): 3652 (m), 3272 (br), 3069 (w), 2952 (w), 2911 (w), 2873 (m), 2846 (w), 1785 (w), 1596 (m), 1557 (s), 1443 (s), 1227 (m), 1162 (w), 1090 (s), 919 (m), 901 (m), 817 (w), 782 (m), 759 (s), 710 (w), 667 (s), 602 (s), 525 (w), 486 (w), 495 (w), 455 (w), 430 (w), 407 (w).

Magnetic measurements:

The magnetic susceptibility measurements were obtained with the use of a Quantum Design SQUID magnetometer MPMS-XL. This magnetometer works between 1.8 and 400 K for dc applied fields ranging from -7 to 7 T. Measurements were performed on polycrystalline samples. ac susceptibility measurements have been measured with an oscillating ac field of 3 Oe and ac frequencies ranging from 1 to 1500 Hz. The magnetic data were corrected for the sample holder. The low-temperature part of the $1/\chi$ vs T curves has been fitted as a straight line, following the Curie-Weiss model $\chi = \mu_{eff}^2/8(T+\Theta)$.

Mössbauer measurements:

The Mössbauer spectra were acquired using a conventional spectrometer in the constant-acceleration mode equipped with a ^{57}Co source (3.7 GBq) in rhodium matrix. Isomer shifts are given relative to α-Fe at room temperature. The sample was inserted inside an Oxford Instruments Mössbauer-Spectromag 4000 Cryostat which has a split-pair superconducting magnet system for applied fields up to 5 T, with the field of the sample oriented perpendicular to the γ - ray direction, while the sample temperature can be varied between 3.0 and 300 K. 3 K temperature could be achieved by pumping the sample space. After the samples were inserted into the cryostat and cooled down to 3K, they were three times warmed up to 50 K and then recooled to 3K. Simulations of Mössbauer spectra were obtained with the program

WMOSS (WMOSS Mössbauer Spectral Analysis Software, www.wmoss.org, 2012-2013) by using the electronic spin-Hamiltonian together with the usual nuclear Hamiltonian for the hyperfine interactions of the ^{57}Fe nuclei:
$\hat{H} = D[\hat{S}_z^2 - 1/3\ S(S+1) + E/D(\hat{S}_x^2 - \hat{S}_y^2)] + \mu_B \cdot S \cdot g \cdot B_o + \hat{S} \cdot A \cdot \hat{I} - g_N \cdot \mu_N \cdot \hat{I} \cdot B_o + eQV_{zz}/4I(2I\text{-}1)[3\hat{I}_z^2 - I^2 + \eta(\hat{I}_x^2 - \hat{I}_y^2)]$, B_o – applied field; $\hat{S} \cdot A \cdot \hat{I}$ is the magnetic hyperfine coupling which connects S and the nuclear spin I, and A is the hyperfine coupling tensor; Q is the quadrupole moment, V_{zz} and η are the main component and the asymmetry parameter of the electric field gradient tensor; all other terms have the standard spin-Hamiltonian meaning.

DFT Calculations. For all four systems the point energy calculations have been performed using the Gaussian 09 programme. [a]. No geometry optimisations were performed, the geometries used were those form X-ray data. The calculations have been performed using the PBE functional [b] and CEP-31G [c] basis set, for the molecules revealing the C_i symmetry. Reoptimisation of the calculated wave functions has been always applied (stable=opt option of Gaussian). For *para*-Me and *meta*-CN system in order to obtain the SCF convergence the temperature broadening during early iterations combined with CDIIS and dynamic damping of early SCF iterations (Fermi keyword of Gaussian) needed to be applied. Tight option of integration was applied.

[a] M. J. Frisch, G. W. Trucks, H. B. Schlegel, G. E. Scuseria, M. A. Robb, J. R. Cheeseman, J. A. Montgomery, Jr., T. Vreven, K. N. Kudin, J. C. Burant, J. M. Millam, S. S. Iyengar, J. Tomasi, V. Barone, B. Mennucci, M. Cossi, G. Scalmani, N. Rega, G. A. Petersson, H. Nakatsuji, M. Hada, M. Ehara, K. Toyota, R. Fukuda, J. Hasegawa, M. Ishida, T. Nakajima, Y. Honda, O. Kitao, H. Nakai, M. Klene, X. Li, J. E. Knox, H. P. Hratchian, J. B. Cross, C. Adamo, J. Jaramillo, R. Gomperts, R. E. Stratmann, O. Yazyev, A. J. Austin, R. Cammi, C. Pomelli, J. W. Ochterski, P. Y. Ayala, K. Morokuma, G. A. Voth, P. Salvador, J. J. Dannenberg, V. G. Zakrzewski, S. Dapprich, A. D. Daniels, M. C. Strain, O. Farkas, D. K. Malick, A. D. Rabuck, K. Raghavachari, J. B. Foresman, J. V. Ortiz, Q. Cui, A. G. Baboul, S. Clifford, J. Cioslowski, B. B. Stefanov, G. Liu, A. Liashenko, P. Piskorz, I. Komaromi, R. L. Martin, D. J. Fox, T. Keith, M. A. Al-Laham, C. Y. Peng, A. Nanayakkara, M. Challacombe, P. M. W. Gill, B. Johnson, W. Chen, M. W. Wong, C. Gonzalez, and J. A. Pople,; Gaussian 09, Revision C.01. Gaussian, Inc., Wallingford CT, 2009.
[b] (1) J. P. Perdew, K. Burke, and M. Ernzerhof, *Phys. Rev. Lett.*, 1996, **77**, 3865. (2) .P. Perdew, K. Burke, and M. Ernzerhof, *Phys. Rev. Lett.*, 1997, **78**, 1396
[c] (1) W.J. Stevens, H. Basch, J. Krauss, *J. Phys. Chem.*, 1984, **81**, 6026. (2) W.J. Stevens, M. Krauss, H. Basch, P.G. Jasien, *Can. J. Chem.* 1992, **70**, 612. (3) T.R. Cundari, W.J. Stevens, *J. Chem. Phys*, 1993, **98**, 5555.

X-Ray Crystallography:

The structures of compounds **1** and **2** have been previously communicated [V. Mereacre, A. Baniodeh, C. E. Anson, A. K. Powell, *J. Am. Chem. Soc.* **2011**, *133*, 15335]; however crystallographic data and refinement details are summarised in Table S1 together with those for **3** and **4**, to aid comparison. Data were measured on Stoe IPDS II image plate diffractometers using graphite-monochromated Mo-Kα radiation, and were corrected for polarisation and absorption. Structure solution (direct methods) and full-matrix least-squares refinement against F^2 (all data) was carried out using the SHELXTL 6.14 software package [G.M. Sheldrick, *Acta Cryst.* **2008**, *A64*, 112]. All ordered non-H atoms were refined anisotropically; disordered atoms were refined isotropically with partial occupancy. Organic H atoms were placed in calculated positions; the positions of H atoms bonded to O were refined with O-H restrained to 0.92(4) Å.
Crystallographic data (excluding structure factors) for the structures published in this paper (**3** and **4**) have been deposited with the Cambridge Crystallographic Data Centre as supplementary publication nos. CCDC 926560 & 926561. The structures of **1** and **2** were previously deposited as CCDC 866243 and 866240, respectively. Copies of the data can be obtained, free of charge, on application to CCDC, 12

Union Road, Cambridge CB2 1EZ, UK: http://www.ccdc.cam.ac.uk/cgi-bin/catreq.cgi, e-mail: data_request@ccdc.cam.ac.uk, or fax: +44 1223 336033.

Table S1. Crystallographic data for compounds **1-4.**

Compound	**1**	**2**	**3**	**4**
Formula	$C_{72}H_{70}Dy_2Fe_2N_{14}O_{20}$	$C_{80}H_{92}Dy_2Fe_2N_4O_{24}$	$C_{64}H_{58}Dy_2Fe_2N_{10}O_{20}$	$C_{66}H_{84}Dy_2Fe_2N_4O_{22}$
FW (g/mol)	1888.12	1930.28	1723.90	1722.07
Crystal system	triclinic	triclinic	triclinic	monoclinic
Space group	P-1	P-1	P-1	$P2_1/c$
a (Å)	11.9912(6)	11.5412(10)	9.700(2)	12.4404(8)
b (Å)	12.8733(7)	14.2757(13)	12.915(3)	21.4830(15)
c (Å)	14.5474(8)	14.4870(12)	14.427(3)	13.7050(9)
α (°)	70.567(4)	61.979(6)	87.159(17)	90
β (°)	79.101(4)	87.646(7)	74.068(18)	100.532(5)
γ (°)	67.143(4)	80.384(7)	73.135(17)	90
V ($Å^3$)	1946.78(18)	2075.5(3)	1662.2(6)	3601.1(4)
Z	1	1	1	2
T (K)	180(2)	200(2)	150(2)	200(2)
Radiation	Mo Kα	Mo Kα	Mo Kα	Mo Kα
F(000)	944	976	856	1736
ρ_{cale} (g/cm^{-3})	1.611	1.544	1.722	1.588
$\mu_{Mo\text{-}K\alpha 1}$ (mm^{-1})	2.341	2.198	2.731	2.521
Crystal size (mm)	0.38×0.33×0.27	0.26×0.21×0.18	0.14×0.11×0.05	0.38×0.33×0.25
Data measured	56533	24227	15190	38489
Unique data	10469	8476	6039	7652
R(int)	0.0465	0.0428	0.0975	0.0808
Data with I>2σ(I)	9443	7303	3726	6012
Parameters	505	517	449	415
wR_2 (all data)	0.0593	0.0972	0.1467	0.1262
S (all data)	1.016	0.999	0.984	1.001
R_1 (I > 2σ(I))	0.0261	0.0400	0.0616	0.0528
Max. diff. peak / hole (e $Å^{-3}$)	+0.88 / -1.08	+0.50 / -2.10	+0.91 / -2.91	+0.68 / -2.64

CCDC	866243	866240	926560	926561

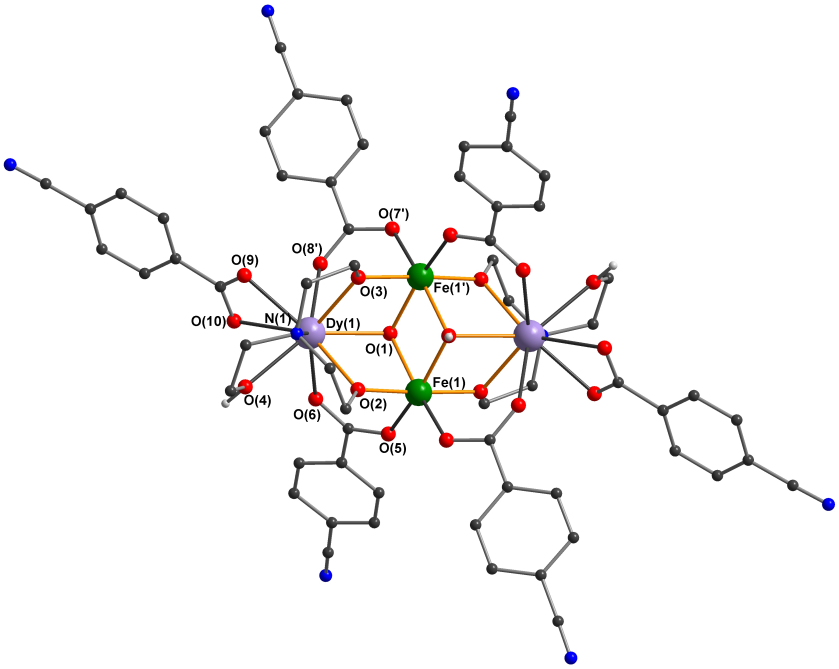

(**1**)

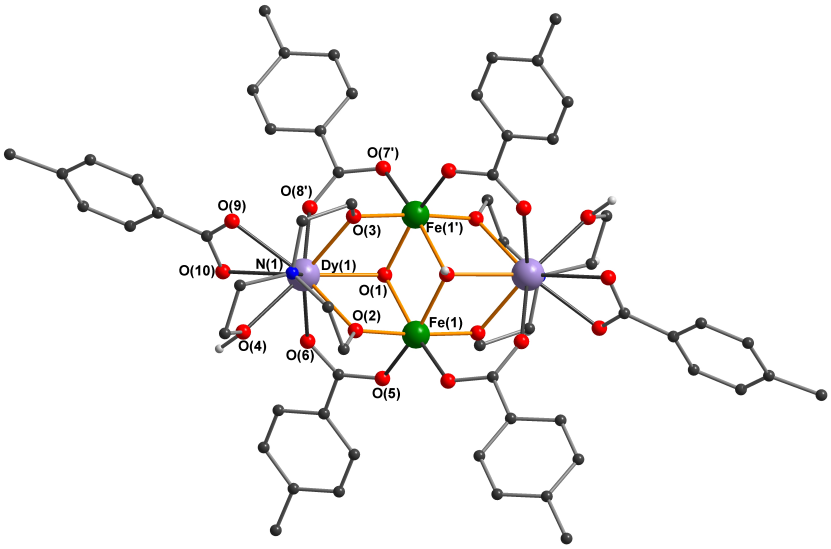

(**2**)

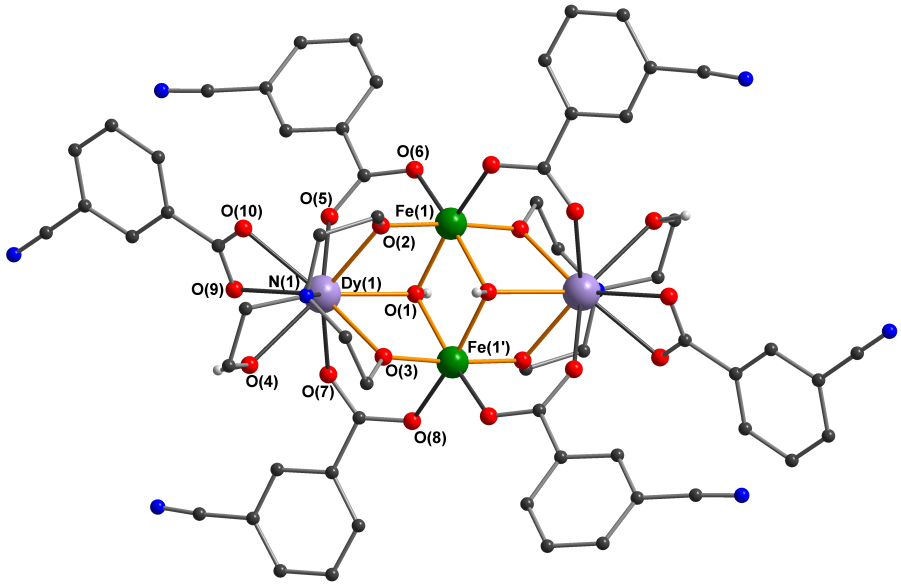

(**3**)

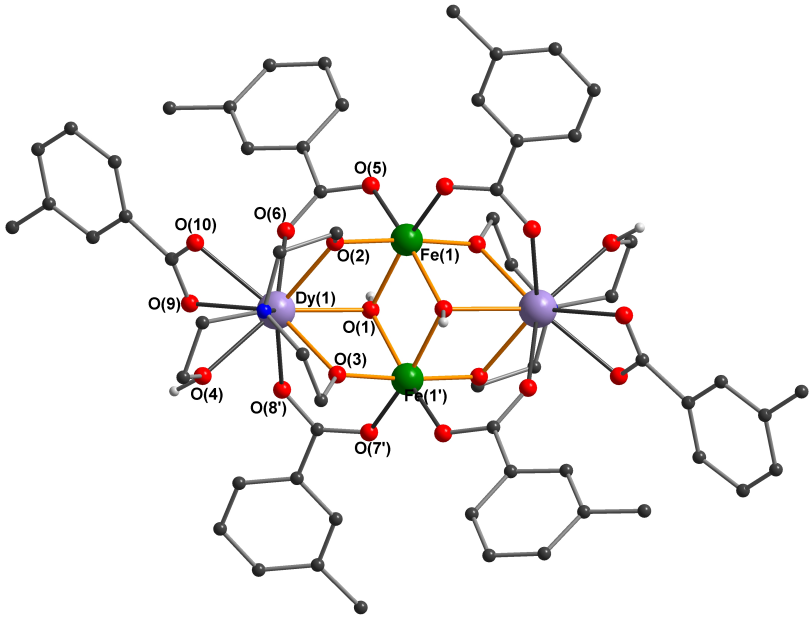

(**4**)

Figure S1. Structures of the Fe_2Dy_2 Clusters in **1-4** (organic H omitted for clarity).

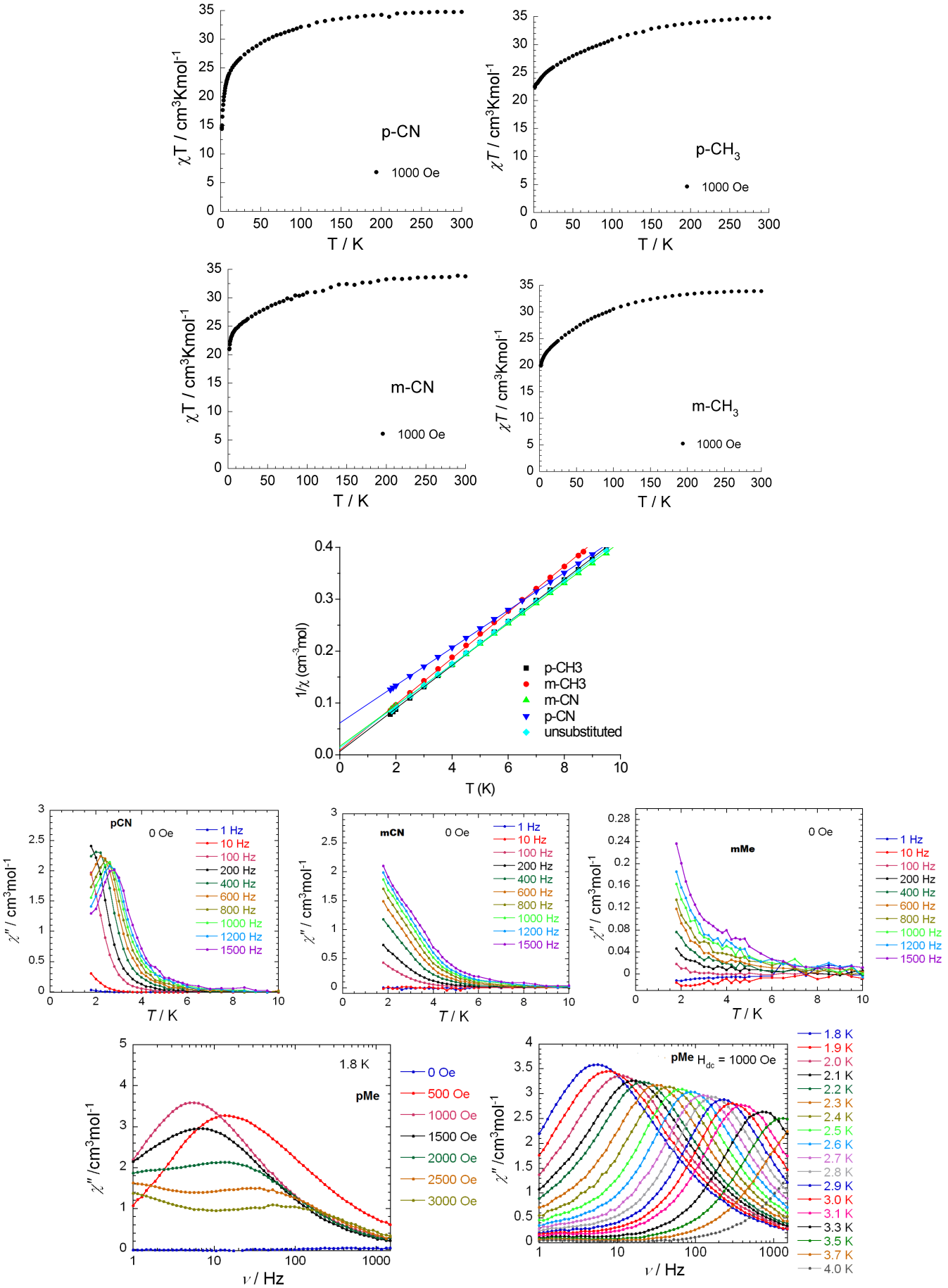

Figure S2. χ_MT versus T plots at 1000 Oe for **1, 2, 3** and **4**; Curie-Weiss fits of the low-temperature 1/χ versus T curves for **1**, **2**, **3**, **4**, and their unsubstituted analog; out-of-phase components of the *ac*-susceptibilities for compounds **1(*p*-CN)**, **3 (*m*-CN)** and **4 (*m*-Me)** at zero-field and different frequencies (top) and for compound **2 (*p*-Me)** at 1.8 K at different fields and at 1000 Oe at different temperatures (bottom).

Table S2. Summary of the magnetic properties of compounds **1-4**.

Compound	Data from *ac*-measurements	Effective barrier	τ_0 (s)
1 (*p*-CN)	*ac*-signal with maxima at 2.5 K	8 K at 0 Oe 13 K at 1000 Oe	$7.68\cdot10^{-6}$ at 0 Oe $2.71\cdot10^{-6}$ at 1000 Oe
2 (*p*-Me)	*ac* signal only present in an applied *dc* field	24.0 K at 1000 Oe	$1.71\cdot10^{-7}$ at 1000 Oe
3 (*m*-CN)	*ac*-signal visible, no maxima without applied *dc* field	22.8 K at 1000 Oe 6.3 K at 2000 Oe	$1.28\cdot10^{-6}$ at 1000 Oe $3.02\cdot10^{-5}$ at 2000 Oe
4 (*m*-Me)	weak *ac*-signal, no maxima without applied *dc* field	21.2 K at 1500 Oe	$5.15\cdot10^{-7}$ at 1500 Oe

Table S3. Mössbauer parameters for compounds **1-4** at 3 K, zero applied field.

		δ,[a] mms^{-1}	ΔE_Q, mms^{-1}	β,[b] °	B_{hf}, T	Γ[c], mms^{-1}	Area, %
1	*p*-CN	0.49(1)	1.06(1)	-	-	0.45(2)	44
		0.49(2)	1.06(1)	35.8	19.9	0.48(2)	56
2	*p*-Me	0.49(1)	0.92(1)	-	-	0.46(1)	70
		0.49(2)	0.92(1)	73.8	5.9	0.36(1)	30
3	*m*-CN	0.49(1)	1.11(1)	-	-	0.48(3)	48
		0.49(2)	1.11(1)	83.3	13.6	0.43(2)	52
4	*m*-Me	0.49(1)	0.94(2)	-	-	0.58(1)	52
		0.49(2)	0.94(2)	53.5	~6.5	0.46(2)	48

[a] The isomer shifts are given relative to α-iron at 295 K.
[b] For magnetically-split spectra the quadrupole shifts are $\varepsilon = \frac{1}{2}\Delta E_Q(3\cos^2\beta-1)$. β - Euler angle between the magnetic hyperfine field B_{hf} and the principal axis of the electrical field gradient (EFG) (V_{zz})
[c] Line width at half maximum.

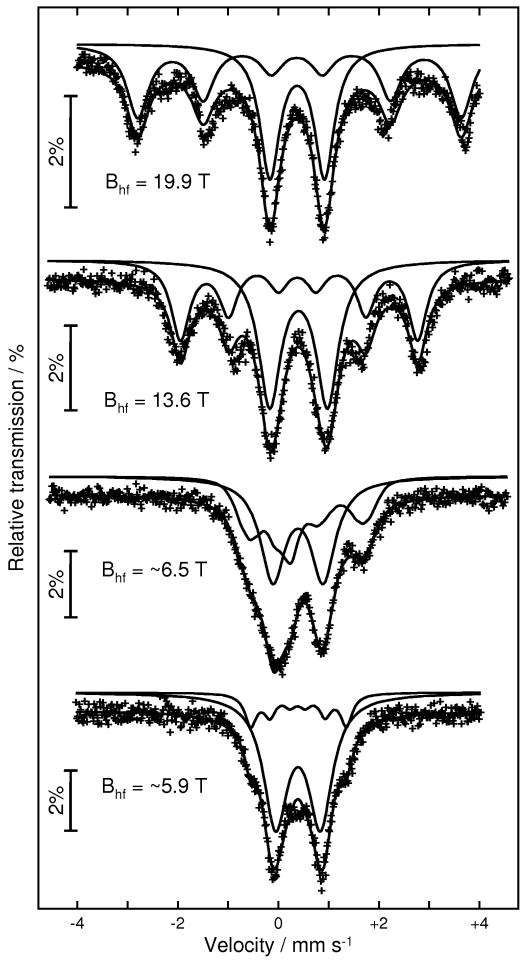

Figure S3. Mössbauer spectra of polycrystalline $[Fe_2Dy_2(OH)_2(teaH)_2(R\text{-}C_6H_4COO)_6]$, where R = *p*-CN, *m*-NC, *m*-Me and *p*-Me at 3 K in zero applied magnetic field (from top to bottom). On left-hand side of every spectrum, the values for the hyperfine field B_{hf} determined from the sextets are given. For compound **4** (R = *m*-Me), the hyperfine field value was extracted from the distribution of probability for the magnetic hyperfine field.

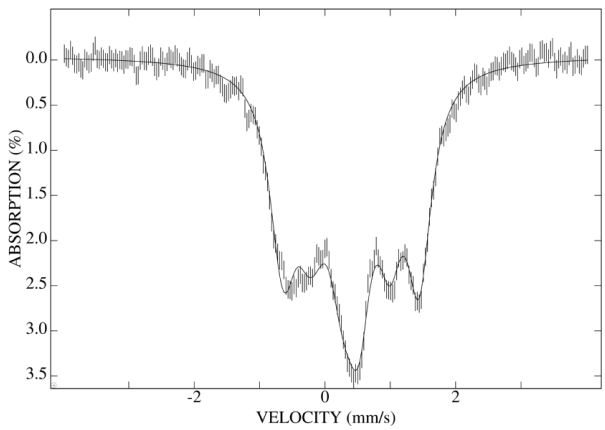

Figure S4. 3 K Mössbauer spectrum of polycrystalline **1** recorded in a perpendicular applied field B_0 of 4.0 T. The solid line is a spectral simulation for ΔE_Q = 1.09 mm/s, δ = 0.50 mm/s, B_{eff} = 4.0 T and η = 1.0, assuming an isolated ground state with S = 0.

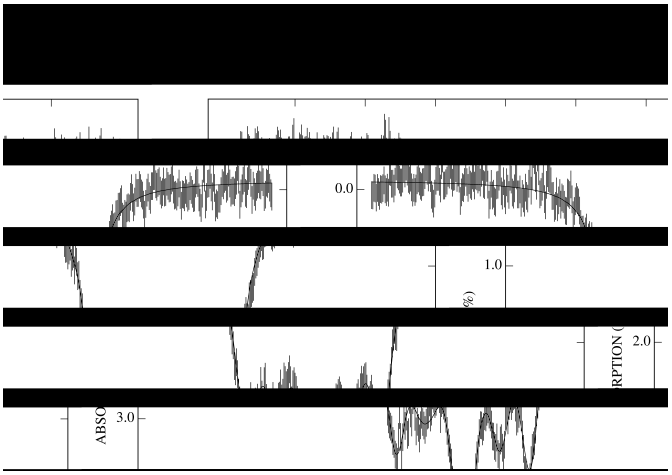

Figure S5. 3 K Mössbauer spectrum of polycrystalline **4** recorded in a perpendicular applied field B_0 of 4.0 T. The solid line is a spectral simulation for ΔE_Q = 0.91 mm/s, δ = 0.49 mm/s, B_{eff} = 4.0 T and η = 1.0, assuming an isolated ground state with S = 0.

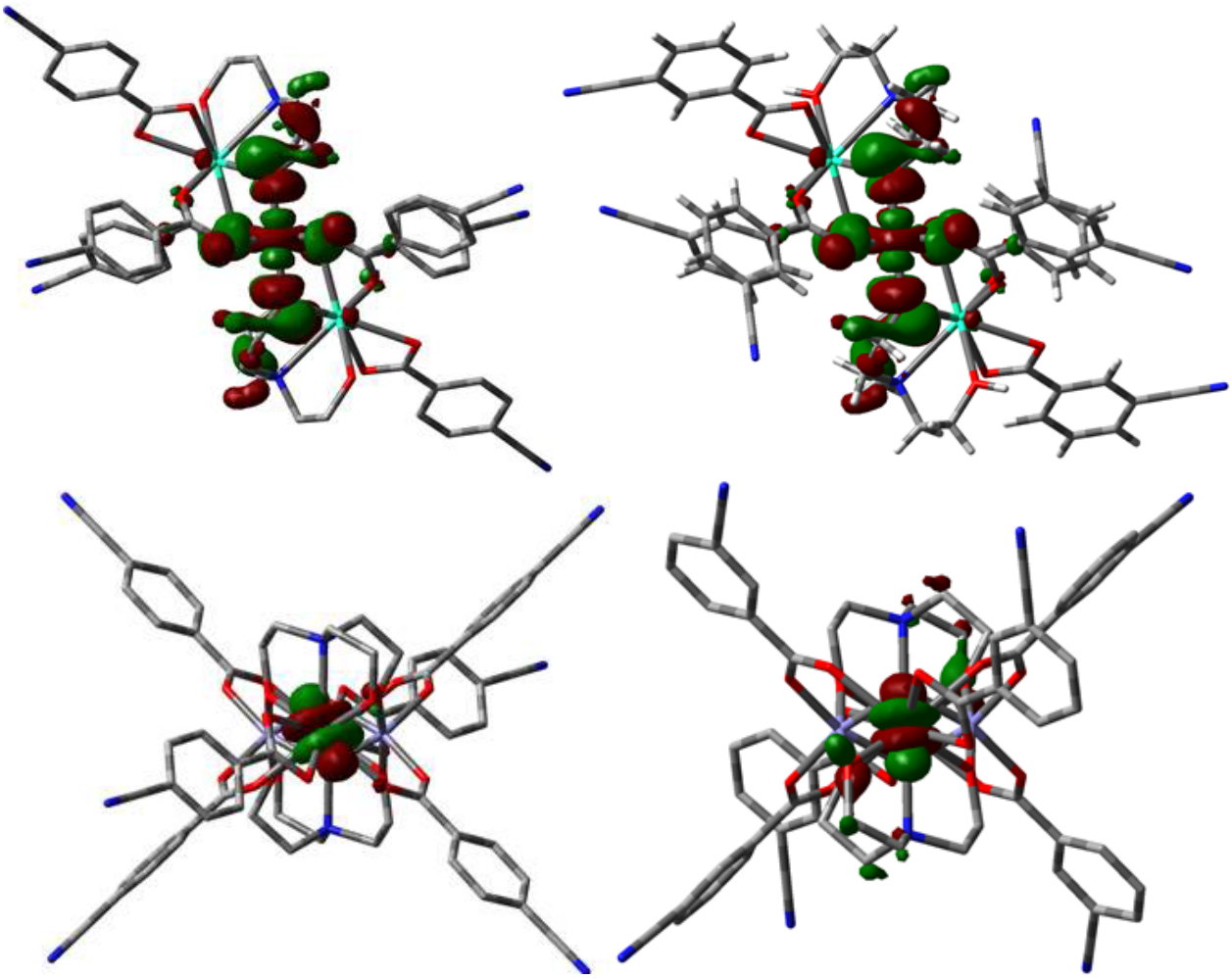

Figure S6. Orientation of Fe $3d_z2$ and Dy $4f_z3$ orbitals relative to the molecular structure for complexes with *p*-CN (**1**) and *m*-CN (**3**) substituted benzoate ligands. *Above*: the HOMO (orbitals with the highest contribution from Fe $3d_z2$) orbitals for **1** (left) and **3** (right). *Below*: the corresponding Dy $4f_z3$ orbitals (orbitals 96 and 95 for **1** (left) and **3** (right)).

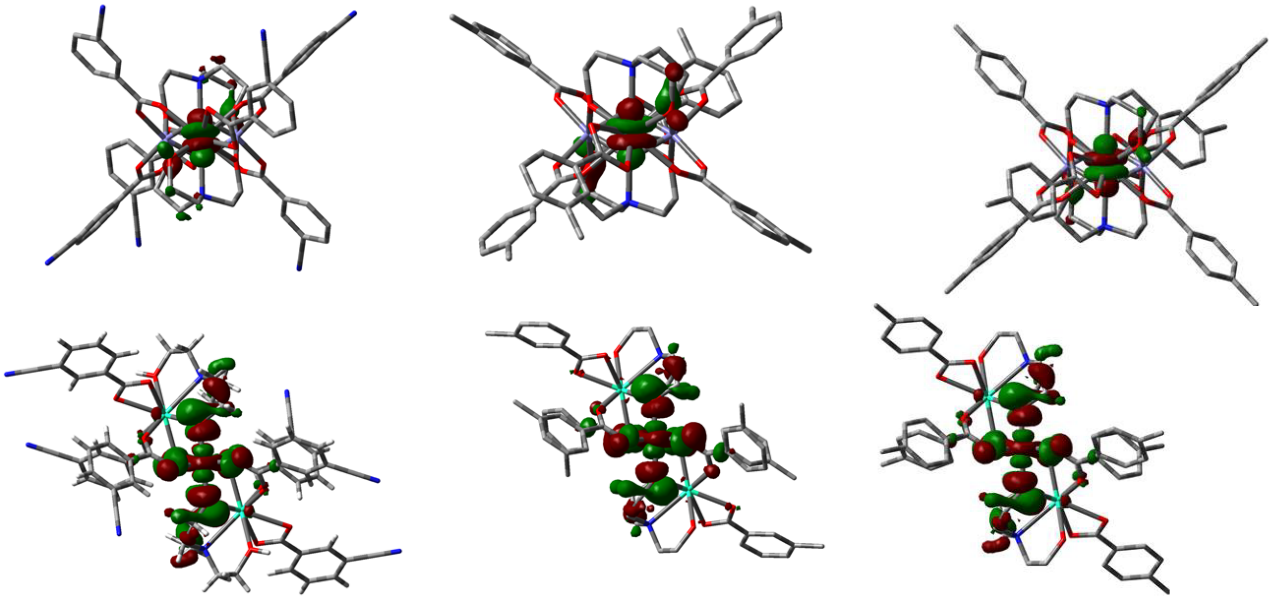

Figure S7. HOMO (bottom) orbitals and 96 orbitals (predominantly Dy ones, top) for *m*-CN (left), *m*-Me (middle) and *p*-Me (right) substituted benzoic acid systems, calculated with DFT (PBE/CEP-31G).

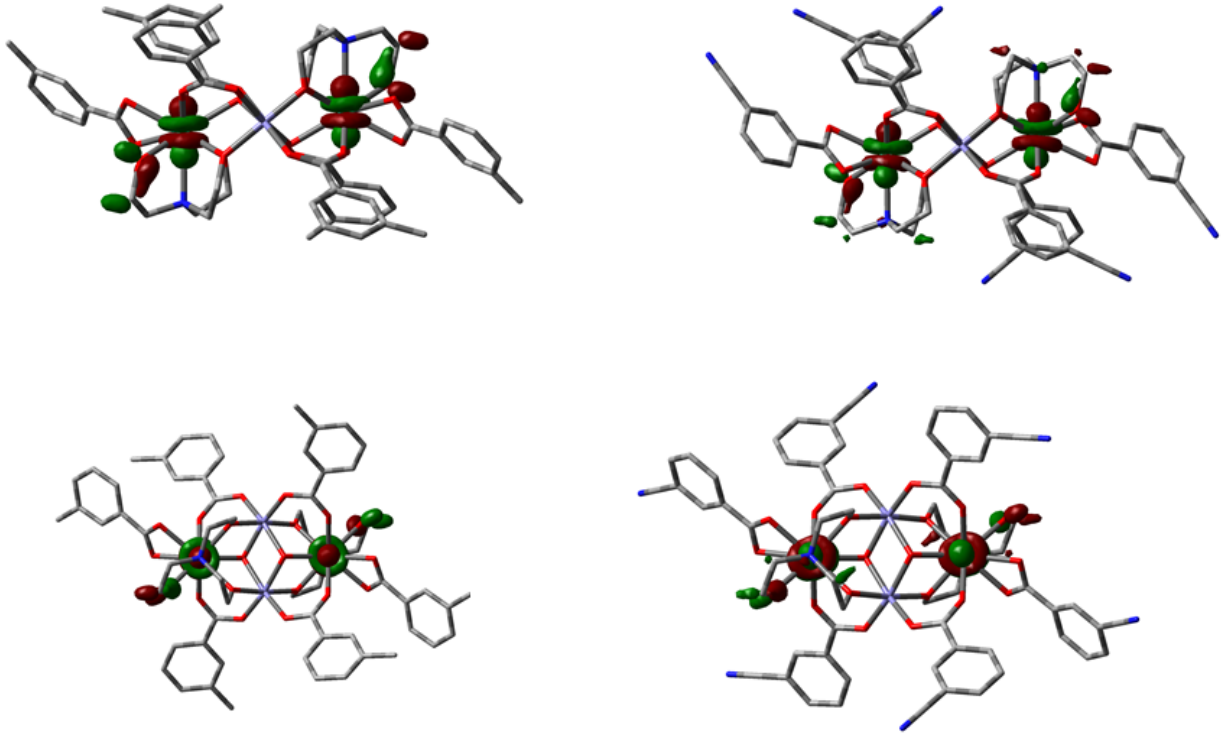

Figure S8. Dy 96 and 95 orbitals of *m*-Me and *m*-CN, with different orientations.